International Journal of Rock Mechanics & Mining Sciences 71 (2014) 381–394

Contents lists available at ScienceDirect

International Journal of Rock Mechanics & Mining Sciences

journal homepage: www.elsevier.com/locate/ijrmms

Size distribution functions for rock fragments

José A. Sanchidrián [a,*], Finn Ouchterlony [b], Pablo Segarra [a], Peter Moser [b]

[a] Universidad Politécnica de Madrid – ETSI Minas, Madrid, Spain
[b] Montanuniversität Leoben, Leoben, Austria

ARTICLE INFO

Article history:
Received 19 October 2013
Received in revised form
7 June 2014
Accepted 6 August 2014
Available online 15 September 2014

Keywords:
Rock fragmentation
Weibull
Swebrec
Grady
Re-scaled
Bimodal

ABSTRACT

The capacity of 17 functions to represent the size distribution of fragmented rock is assessed on 1234 data sets of screened fragments from blasted and crushed rock of different origins, of sizes ranging from 0.002 to 2000 mm. The functions evaluated are Weibull, Grady, log-normal, log-logistic and Gilvarry, in their plain, re-scaled and bi-component forms, and also the Swebrec distribution and its bi-component extension. In terms of determination coefficient, the Weibull is the best two-parameter function for describing rock fragments, with a median R^2 of 0.9886. Among re-scaled, three-parameter distributions, Swebrec and Weibull lead with median R^2 values of 0.9976 and 0.9975, respectively. Weibull and Swebrec distributions tie again as best bi-component, with median R^2 of 0.9993. Re-scaling generally reduces the unexplained variance by a factor of about four with respect to the plain function; bi-components further reduce this unexplained variance by a factor of about two to three. Size-prediction errors are calculated in four zones: coarse, central, fines and very fines. Expected and maximum errors in the different ranges are discussed. The extended Swebrec is the best fitting function across the whole passing range for most types of data. Bimodal Weibull and Grady distributions follow, except for the coarse range, where re-scaled forms are preferable. Considering the extra difficulty in fitting a five-parameter function with respect to a three-parameter one, re-scaled functions are the best choice if data do not extend far below 20% passing. If the focus is on the fine range, some re-scaled distributions may still do (Weibull, Swebrec and Grady, with maximum errors of 15–20% at 8% passing), but serious consideration should be given to bi-component distributions, especially extended Swebrec, bimodal Weibull and bimodal Grady.

1. Introduction

The assessment of fragmentation by blasting and the subsequent crushing and grinding is an important issue in mining. Operation control and optimization require the description of size distributions in several stages, as fragmentation characteristics influence the mucking productivity, the crusher throughput and energy consumption, the plant efficiency, yield and recovery, and the price itself of the end product in the case of industrial minerals and aggregates. Models, specifications and process data of fragmentation by blasting [1–9], crushers, mills, screens, belts, mineral ducts, bins, cyclones, and plant operation in general [10–20] use distribution functions. However, the domain of sizes or fractions passing in which a given distribution function does really represent the rock fragment size is often neglected. This work tackles this point by examining the errors that can be expected across a broad percent passing range when rock fragmentation is described by different distribution functions.

Rock fragment sizes have been represented for many years, almost exclusively, by means of the Rosin–Rammler (or Weibull) distribution [21–23]; in the last several years, the recently developed Swebrec function [24,25] has gained a relatively high profile as it has been shown to represent the fragmented rock sizes with advantage over the Weibull both in the fines and in the coarse ends. Djordjevic [6] used bimodal Weibull for describing rock fragmented by blasting and Blair [26] studied the behavior of the lognormal and log-logistic bimodals for the same purpose. A wider comparison of functions, namely the Weibull, Swebrec, Grady [27,28] and Gilvarry [29–32], and their bi-component varieties was presented in 2009 [33], with a limited number (28) of data sets. That methodology was applied [34] to a much larger data base, made up of 448 sets of screened fragment size data of rock of a variety of origins and fragmentation processes; the lognormal and its bi-component were also included at that point among the distributions analyzed.

The errors in predicting sizes were determined for each of the distribution functions across the range of data, dividing the passing range in four zones: coarse (> 80%), central (80–20%), fine (20–2%) and very fine (< 2%). Swebrec was by far the best single component function in all zones, with errors comparable to

* Corresponding author. Tel.: +34 913367060.
E-mail address: ja.sanchidrian@upm.es (J.A. Sanchidrián).

http://dx.doi.org/10.1016/j.ijrmms.2014.08.007
1365-1609/

the best bi-components in the coarse and central. Indeed, it is not surprising that a three-parameter function such as the Swebrec outdoes two-parameter ones like Weibull, Grady and lognormal, and raises the question of how the latter ones (for which the independent variable x covers the semi-infinite interval $0 \le x < \infty$) would behave if a re-scaled, finite-interval-transformed form of them (including as third parameter a maximum size, as Swebrec does) were employed. This matter has also been addressed [35] by comparing single, plain functions with their re-scaled variants, and with the Swebrec function itself. The most relevant outcome of that study was that the re-scaled Weibull matched Swebrec as best distributions fitting the four ranges.

The present work extends the comparison to re-scaled vs. bi-component distributions, in an exercise to assess the benefits of the increased number of parameters of the latter, which complicates the fitting problem even with state-of-the-art routines. As work progressed, the experimental data base nearly tripled from the 448 data sets in [34,35], to 1234 in the present paper, thereby improving the statistical significance and giving the conclusions a greater validity.

2. The functions

Table 1 lists the distributions tested; their expressions are given below in their cumulative distribution function (CDF) form, F.

2.1. Plain, single-component:

Weibull–Rosin–Rammler (abbreviated here WRR [21–23]):

$$F_{WRR} = 1 - \exp[-(x/x_c)^n], \quad 0 \le x < \infty \tag{1}$$

where x_c and n are the scale and shape parameters, respectively.

Grady (abbreviated GRA [27,28]):

$$F_{GRA} = 1 - [1 + (x/x_g)^\alpha]\exp[-(x/x_g)^\alpha], \quad 0 \le x < \infty \tag{2}$$

where x_g and α are the scale and shape parameters, respectively.

Lognormal (LGN):

$$F_{LGN} = \Phi[(\log x - x_m)/s], \quad 0 \le x < \infty \tag{3}$$

where Φ is the standard normal cumulative distribution; x_m and s are the location and scale parameters (the mean and the standard deviation of the natural logarithm of x).

Log-logistic (LGL):

$$F_{LGL} = \frac{1}{1 + (x/x_{50})^{-\gamma}}, \quad 0 \le x < \infty \tag{4}$$

where x_{50} (the median size) and γ are the scale and shape parameters, respectively.

Gilvarry (GIL [29–32]):

$$F_{GIL} = 1 - \exp\{-[(x/x_1) + (x/x_1)^2 + (x/x_1)^3]\}, \quad 0 \le x < \infty \tag{5}$$

where x_1, x_2 and x_3 are first, second and third order scale parameters.

2.2. Re-scaled

The distributions in Eqs. (1)–(5), which reach the unit value only at infinite size, can be transformed by scaling the abscissa with a maximum size x_{max} and forcing an infinite value of the variable at that point, thereby bringing the function value to 1; this is accomplished by substituting ξ for x:

$$\xi = \frac{(x/x_{max})}{1 - (x/x_{max})} = \frac{x}{x_{max} - x}, \quad 0 \le x \le x_{max} \tag{6}$$

The resulting function $F_T(\xi)$, with a semi-infinite $(0 \le \xi < \infty)$ domain, is thus transformed into a finite x domain $(0 \le x \le x_{max})$ when expressed in the form $F_T(x)$. As an example, the re-scaled Weibull distribution is, from Eqs. (1) and (6):

$$F_{TWRR} = 1 - \exp[-(\xi/\xi_c)^n] = 1 - \exp\{-[x(x_{max} - x_c)/x_c(x_{max} - x)]^n\}, \quad 0 \le x \le x_{max} \tag{7}$$

Similarly for the other distributions. Re-scaling transformed functions are referred here with the parent function acronym preceded by a T; they have one more parameter (x_{max}) than the original function.

One more re-scaled distribution, without a semi-infinite counterpart, is the Swebrec (SWE [24,25]):

$$F_{SWE} = \frac{1}{1 + [\log(x_{max}/x)/\log(x_{max}/x_{50})]^b}, \quad 0 \le x \le x_{max} \tag{8}$$

where x_{50} is the scale parameter (median size) and b a shape parameter.

2.3. Bi-component

Bi-component functions, usually representing bi-modal distributions, can be formed as a linear combination of two single-component ones as follows:

$$F_{Bi} = (1 - f)F(x, \overline{\pi}_1) + fF(x, \overline{\pi}_2), \quad 0 \le x < \infty \tag{9}$$

where F is any of the functions in Eqs. (1)–(5); $f (0 \le f \le 1)$ is the fraction of the modality with a parameter set $\overline{\pi}_2$, so that $1–f$ is the fraction of the modality $\overline{\pi}_1$. For example, the bi-component log-logistic is

$$F_{BiLGL} = (1 - f)F_{LGL} + fF_{LGL} = (1 - f)\frac{1}{1 + (x/x_{50,1})^{-\gamma_1}} + f\frac{1}{1 + (x/x_{50,2})^{-\gamma_2}}, \quad 0 \le x < \infty \tag{10}$$

Bi-component functions are referred here with the parent single component function acronym preceded by Bi. The BiWRR was used by Djordjevic [6] in his two-component model of blast fragmentation; the BiLGN and BiLGL have been used by Blair [26].

For the Swebrec case, a so-called extended version (ExSWE) exists [24,25] similar to the bi-components but, like its single component sister, of re-scaled character:

$$F_{ExSWE} = \frac{1}{1 + a[\log(x_{max}/x)/\log(x_{max}/x_{50})]^b + (1 - a)[((x_{max}/x) - 1)/((x_{max}/x_{50}) - 1)]^c}, \quad 0 < x \le x_{max} \tag{11}$$

whose behavior at large x is that of Eq. (8) and at small x is that of a power distribution with exponent c; a is a partition coefficient similar to f in Eq. (9).

Table 1
Distribution functions.

Distribution	Domain	No. of parameters	Acronym
Weibull or Rosin–Rammler	Semi-infinite $[0, \infty)$	2	WRR
Grady	Semi-infinite $[0, \infty)$	2	GRA
Lognormal	Semi-infinite $[0, \infty)$	2	LGN
Log-logistic	Semi-infinite $[0, \infty)$	2	LGL
Gilvarry	Semi-infinite $[0, \infty)$	3	GIL
Re-scaled Weibull	Finite $[0, x_{max}]$	3	TWRR
Re-scaled Grady	Finite $[0, x_{max}]$	3	TGRA
Re-scaled lognormal	Finite $[0, x_{max}]$	3	TLGN
Re-scaled log-logistic	Finite $[0, x_{max}]$	3	TLGL
Swebrec	Finite $[0, x_{max}]$	3	SWE
Re-scaled Gilvarry	Finite $[0, x_{max}]$	4	TGIL
Bi-component Weibull	Semi-infinite $[0, \infty)$	5	BiWRR
Bi-component Grady	Semi-infinite $[0, \infty)$	5	BiGRA
Bi-component lognormal	Semi-infinite $[0, \infty)$	5	BiLGN
Bi-component log-logistic	Semi-infinite $[0, \infty)$	5	BiLGL
Extended Swebrec	Finite $[0, x_{max}]$	5	ExSWE
Bi-component Gilvarry	Semi-infinite $[0, \infty)$	7	BiGIL

Table 2
Fragmentation data.

Mine or quarry site, or rock origin	Rock	No. of sets	Ref.	n_p	x_{min} (mm)	x_{max} (mm)	p_{min} (%)
(a) Blasted material							
1. *Blasted, mine* (*202 data sets*)							
El Alto, Spain	Limestone	1	[36]	16	0.063	800	0.36
Christmas mine, USA	Copper ore	3	[37]	10	19.05	381	12.1–19.9
Mt. Coot-tha, Australia	Hornfel	1	[38]	24	0.355	2000	2.75
Bårarp, Sweden	Granite	7	[39]	19–20	0.075	500–1000	0.1–0.6
Kållered, Sweden	Gneiss	6	[40]	17	0.075	2000	0.34–0.49
Billingsryd, Sweden	Dolerite	6	[40]	18	0.074	2000	0.76–1.03
South Africa	Gold reef	8	[41]	8–26	0.053–0.075	300–304	0.16–3.1
South Africa	Granite	17	[41]	7	10	500	4.7–12.5
Rolla, USA	Dolomite	29	[4]	6–8	9.525	228.6–457.2	7.9–20.6
Stewartsville, USA	Dolomit. limestone	20	[42]	7–8	4.7625	228.6–558.8	1.03–3.86
Not reported	Rhyoporphyry	8	[43]	11	100	1500	4.7–11.4
Kiruna	Magnetite	16	[44]	5	10	500	10.1–36.8
Kiruna	Magnetite[a]	39	[45]	6–14	0.074–10	4.7–800	1.39–42.5
Rolla, USA	Dolomite	19	[46]	7–8	4.7625	304.8–609.6	2.8–7.4
Kiruna	Magnetite[b]	12	[47,48]	18–25	0.063	40–800	0.69–7.6
Kopanang, South Africa	Carbonized gold reef	10	[49]	10–12	0.075	150–250	0.27–3.8
2. *Blasted, specimens* (*534 data sets*)							
Not reported	Limestone	1	[50]	15	0.002	203	0.004
Darley Dale, UK	Sandstone	12	[50]	16	0.002	406	0.003–0.03
Imberg, Germany	Sandstone	3	[51]	19–21	0.063	80–125	0.13–0.45
Eibenstein, Austria	Amphibolite	15	[52]	14–20	0.063	25–125	0.14–3.5
Bårarp, Sweden	Granite	7	[39,53]	15–21	0.063	31.5–125	0.21–3.2
El Alto, Spain	Limestone	12	[52]	14–21	0.063	25–125	0.13–4.0
Klinthagen, Sweden	Limestone-stroma[c]	9	[52]	15–20	0.063	31.5–100	0.18–1.9
Klinthagen, Sweden	Limestone-crin[c]	9	[52]	13–21	0.063	20–125	0.16–1.9
Klinthagen, Sweden	Limestone-mass[c]	9	[52]	14–21	0.063	25–125	0.20–2.7
Klinthagen, Sweden	Limestone-frag[c]	10	[52]	13–20	0.063	20–100	0.32–3.4
Norway	Syenite, granite, gabbro, gneiss	21	[54,55]	9–11	0.25–0.50	100–150	0.06–1.8
Artificial	Magnetite concrete	86	[56]	7–13	0.063–0.212	11.3–128	0.26–17.6
Artificial	Cement mortar	3	[57,58]	12	0.075	128	0.10–0.17
Not reported	Limestone	69	[59]	7–8	0.6	40–80	0.3–4.7
Not reported	Cement mortar, Granite	95	[60]	4–8	3.33	25.4–76.2	0.3–42.7
Klinthagen, Sweden	Limestone	14	[61]	7–9	0.212	16–64	0.1–9.1
Kiruna, artificial	Magnetite and magnetic mortar	131	[62]	14–17	0.06–0.125	45–125	0.01–3.2
Artificial	Magnetic mortar	28	[63]	14–15	0.063	90–125	0.13–0.9

Mine or quarry site, or rock origin	Rock, equipment	No. of sets	Ref.	n_p	x_{min} (mm)	x_{max} (mm)	p_{min} (%)
(b) Crushed and milled material-plant							
3. *Primary, secondary and tertiary crusher, plant* (*116 data sets*)							
El Alto, Spain	Limestone, toothed roller crusher	1	[36]	17	0.063	63	1.1
Kållered, Sweden	Gneiss	10	[40]	14	0.074	40	4.9–7.4
Tampomas, Indonesia	Andesite, jaw crusher	2	[64]	20–21	0.075	200–300	0.47–1.1
Klinthagen, Sweden	Limestone, toothed roller crusher	28	[65]	9–18	0.063–8	200–300	0.13–18.8
Not reported	Crusher	1	[13]	10-10	1.18	31.5	11.2
Norway	Anorthosite, gyratory crusher	4	[55,66]	12	0.075	32	0.60–0.81
Tampomas, Indonesia	Andesite, gyratory crusher	15	[64]	16–20	0.075	63–200	0.20–1.6
Tampomas, Indonesia	Andesite[d]	31	[64]	8–18	0.075–9.5	28–100	0.04–4.4
Aitik, Sweden	Porphyry copper ore. Crusher	24	[67]	8–11	4–16	200–300	4.8–37.7
4. *Milling and grinding, plant* (*48 data sets*)							
Tampomas, Indonesia	Andesite, rod mill	9	[64]	9–12	0.075	6.3–19	1.05–6.2
Not reported	AG mill	1	[13]	12	0.038	1.4	23.3
Not reported	Hydrocyclone overflow	1	[13]	12	0.009	0.3	19.5
McCoy mine, USA	Limestone, single particle roll mill	16	[68–70]	12	0.074	3.36	4.1–12.7
McCoy mine, USA	Limestone, ball mill	16	[68,69]	11–12	0.074	2.38–3.36	8.3–34.6
Kiruna, Sweden	Crude ore, fully autogenous mill circuit	4	[71,72]	8–24	0.045–3.3	100	7.3–48.8
Keewatin, MN, USA	Iron ore, SAG feed	1	[73]	21	0.15	200	2.8
5. *Crushing, milling and grinding, laboratory* (*82 data sets*)							
Eibenstein, Austria	Amphibolite[e]	13	[74]	5–13	0.04	1–40	0.57–18.6
El Alto, Spain	Limestone[e]	5	[74]	5–13	0.04	1–40	0.46–11.7
Klinthagen, Sweden	Limestone-stroma[e,f]	5	[74]	5–13	0.04	1–40	0.98–14.0
Klinthagen, Sweden	Limestone-crin[e,f]	5	[74]	5–13	0.04	1–40	0.91–16.9
Klinthagen, Sweden	Limestone-mass[e,f]	5	[74]	5–13	0.04	1–40	0.94–14.6
Klinthagen, Sweden	Limestone-frag[e,f]	5	[74]	5–13	0.04	1–40	2.0–16.2
Kiruna, Sweden	Magnetite	10	[75]	4–16	0.063	0.5–31.5	0.48–25.6
Five sites, Virginia, USA	Several, igneous and siltstone, jaw crusher	8	[76]	4–6	2.36–4.75	19.1–35.92	0.56–17.8
Not reported	Magnetite, lab crusing circuit	1	[77]	17	0.037	3.35	2.24
Five mine sites, Turkey	Chromite ore run-of-mine; output of jaw, cone, hammer crushers and ball mill	25	[78]	12–18	0.038	1–12.7	0.8–17.5
6. *Single-particle, inter-particle, drop-weight, impact, compression crushing* (*238 data sets*)							
Kiruna, Sweden	Magnetite, single-particle and inter-particle crushing	39	[79]	9–10	0.25	16–19	0.18–16.4
Kiruna, Sweden	Magnetite, drop weight breakage	6	[80]	18–25	0.045	13.3–50.8	0.12–1.5

Table 2 (*continued*)

Mine or quarry site, or rock origin	Rock, equipment	No. of sets	Ref.	n_p	x_{min} (mm)	x_{max} (mm)	p_{min} (%)
Brasil	Gneiss, granulite, granitiods, single –particle breakage	27	[81]	13–21	0.053–0.85	3.35–90	0.8–10.5
Japan	Marble, sandstone, tuff, andesite, dolomite, uniaxial compression test	24	[82]	12–14	0.177	25.4–50.8	1.8–21.8
Five sites, Virginia, USA	Several, igneous and siltstone, high energy crushing test	14	[76]	18	0.075	38.1	0.06–1.9
-	Monzonite, wollastonite, siltstone, Impact crushing	45	[83,84]	14–15	0.037–0.053	4.76	0.11–4.8
Kiruna	Magnetite run-of-mine, inter-particle breakage	9	[85]	12–13	0.063	19–22	0.15–2.1
Kiruna	Magnetite run-of-mine, inter-particle breakage	8	[86]	12	0.063	19	0.20–1.5
Not reported	Magnetite, projectile impact	66	[77]	5–15	0.037–0.15	0.15–2	0.20–75.9
7. *Shock release fragmentation* (*14 data sets*)							
Northern Eldorado Mountains, Nevada, USA	Volcanoclastic sandstone	14	[87]	13–17	0.0442	4–64	0.02–9.5

[a] Twelve data sets are screening of fines (< 10 mm), given as separate curves.
[b] Six data sets are screening of fines (< 63 mm), given as separate curves.
[c] Limestone qualities in Klinthagen. Stroma: stromatoporoid; crin: crinoidal; mass: massive reef; frag: fragmented.
[d] Different materials sampled in the crushing plant have been included in this group: gyratory crusher product mixed with cone crusher recycled product, impact crusher feed (cone product partially sieved off) and product, and product partially sieved off (feed to a rod mill).
[e] Steiner's [88] "optimized comminution sequences", consisting of several stages of crushing and milling with a small scale reduction plus classification and feedback.
[f] Limestone qualities in Klinthagen. Stroma: stromatoporoid; crin: crinoidal; mass: massive reef; frag: fragmented.

3. The data

Previous work [34,35] comprised 448 rock fragmentation data sets of varied nature and fragmentation method: blasting in mine, blasting in lab-scale blocks, crushing, grinding and milling both from mine plants and laboratory tests. Since then, more data sets of these types have been added, and other fragmentation mechanisms have been included: single-particle and inter-particle breakage, drop-weight crushing, impact crushing, compression test and shock decompression, making a total of 1234 data sets. All of them are sieved and weighed values. Table 2 gives the sources and a basic description of the data; n_p is the number of points per data set, x_{min} and x_{max} are the minimum and maximum sizes, and p_{min} is the minimum percent passing of the data.

Table 3 gives extremes and medians of some descriptive parameters of the data sets: coefficient of variation (CV, ratio of standard deviation to mean), skewness, kurtosis, log-passing range, log-size range and overall log-slope. The last three are defined as follows: Log-size range: $r_x = \log_{10}(x_{max}/x_{min})$; Log-passing range: $r_p = \log_{10}(p_{max}/p_{min})$; overall log-slope: $s_L = r_p/r_x$.

The distributions of these parameters are also shown graphically as box-plots in Fig. 1. The log-slope (since it refers to the slope of a cumulative distribution) is a dispersion measure additional to the coefficient of variation, with an inverse relation to it: a steep CDF (high slope) generally means a small dispersion. Skewness and kurtosis are also mutually related, as usually happens with skewed distributions, where higher absolute values of skewness encompass higher kurtosis (e.g. groups 1, 4 and 7). The data sets are generally positively skewed (right-tailed), and only group 5 has a large proportion of negatively skewed data.

Clustering of the data has been tried, aimed at merging some of the groups, using the above descriptors. Both hierarchical tree clustering and *k*-means methods have been conducted; clusters obtained never shape from distinct groups but are always combinations of elements from several of them, resulting in the groups divided into the clusters. This means that the groups themselves are not homogeneous structures of data in terms of the statistical descriptors; however, it was not our intention, at this stage, to make a different grouping of the data but only to check if some of the groups could be reasonably lumped together in order to simplify the number of categories of data (seven), for further analysis. In an additional attempt, the Mann–Whitney rank sum test was performed on the above-mentioned descriptors. For each pair of groups, the hypothesis that the distributions of a descriptor in both groups are identical with equal medians is assessed. The result is summarized in Table 4, where the parameters shown are the ones for which the comparison test does not reject the hypothesis of equal distributions to a 0.05 significance. No pair of groups has equal distributions for all parameters; noticeably, the main descriptive statistics (CV, skewness and kurtosis) of group 7 (shock release fragmentation) appear to be congruent (i.e., the hypothesis of equal distributions is not rejected) with those of group 1 (blasted, mine) with quite strong *p*-values. Since the amount of data sets from shock decompression is small (14), preventing to draw any statistically significant conclusions on it alone, it was decided to include these data sets in the blasting, mine, group.

Table 3
Descriptive statistics of the data. For each group and descriptor, maximum, median and minimum values are given.

		CV	s_L	r_p	r_x	Skewness	Kurtosis
Group 1	Max	1.45	1.13	2.88	4.43	2.88	9.08
	Med	0.78	0.56	1.16	1.90	1.07	0.56
	Min	0.46	0.21	0.37	1.18	−0.25	−1.44
Group 2	Max	1.36	1.83	4.45	5.31	2.45	15.20
	Med	0.61	0.79	1.93	2.55	0.39	−0.45
	Min	0.17	0.35	0.37	0.88	−3.86	−1.68
Group 3	Max	1.06	2.86	3.40	3.68	1.64	2.85
	Med	0.71	0.61	1.50	2.73	0.48	−0.78
	Min	0.38	0.35	0.42	1.02	−0.37	−1.74
Group 4	Max	1.31	0.84	1.98	3.35	6.35	53.94
	Med	0.76	0.57	1.02	1.66	1.34	2.44
	Min	0.51	0.21	0.31	1.48	−0.37	−1.47
Group 5	Max	0.99	2.91	2.34	3.00	1.25	2.76
	Med	0.59	0.66	1.42	2.05	−0.03	−1.08
	Min	0.16	0.47	0.59	0.73	−0.90	−1.47
Group 6	Max	1.46	2.52	3.22	3.05	2.38	20.60
	Med	0.71	0.76	1.57	1.95	0.49	−0.44
	Min	0.09	0.11	0.12	0.61	−3.41	−1.58
Group 7	Max	1.45	1.16	3.67	3.16	4.70	27.57
	Med	0.74	0.66	1.51	2.18	0.98	0.72
	Min	0.58	0.49	1.02	1.96	−0.49	−1.29
All	Max	1.46	2.91	4.45	5.31	6.35	53.94
	Med	0.66	0.71	1.64	2.12	0.53	−0.40
	Min	0.09	0.11	0.12	0.61	−3.86	−1.74

4. The fits

The 17 distributions described in Section 2 have been fitted to the 1234 data sets using an ordinary least squares scheme. Where the passing interval is wide, a weighed least squares scheme is often appropriate, as ordinary least squares fits tend to match the coarse zone and neglect the rest [33]. The weighting function depends on the range of sizes and passing of interest, and typically

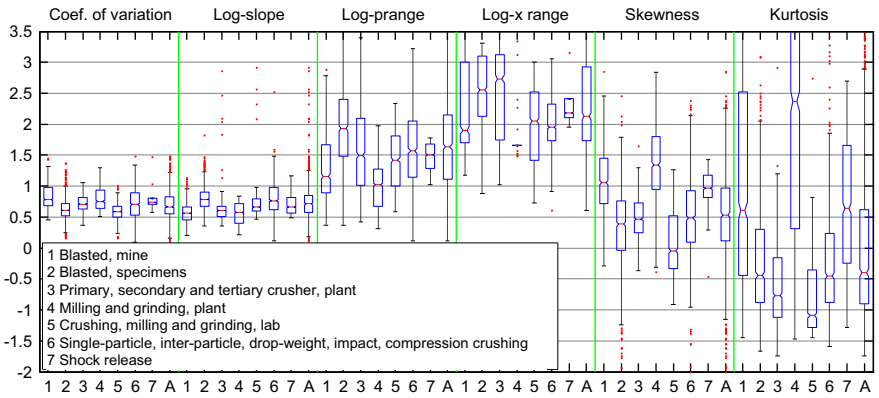

Fig. 1. Descriptors of the data sets. Numbers 1–7 in the horizontal axis indicate each of the categories in Table 2, also shown in the legend; "A" indicates distributions for all the data sets. Whiskers extend up to 1.5 times the interquartile range;beyond that, data are represented as red points. (For interpretation of the references to color in this figure legend, the reader is referred to the web version of this article.)

Table 4
Comparison of descriptors of the various groups of data; shown are those whose distributions for each pair of data groups may not be different (i.e. the Mann–Whitney rank-sum test does not reject the hypothesis of equal distributions to a 0.05 significance); *p*-values of the test are shown.

	1	2	3	4	5	6	7
1	All	–	r_x	CV/s_L	r_p/r_x	r_x	CV/skew/kurt
	1		0.10	0.19/0.97	0.06/0.38	0.60	0.35/0.47/0.80
2		All	r_x	–	CV	s_L/kurt	s_L/r_x
		1	0.64		0.10	0.36/0.92	0.16/0.06
3			All	s_L	–	CV/skew/r_p	CV/$s_L/r_p/r_x$
			1	0.28		0.95/0.83/0.87	0.26/0.78/0.55/0.09
4				All	–	–	CV/kurt
				1			0.85/0.08
5					All	r_x	s_L/r_p
					1	0.85	0.33/0.90
6						All	CV/s_L/r_p
						1	0.34/0.95/0.28
7							All
							1

an inverse function of the size or the passing is used [33,89]. The form of the weighing function is in itself an important subject [33] which, for the sake of conciseness, is not discussed in the present paper.

The fitting code has been programmed in Matlab [90] using non-linear minimization routines. Two types of algorithms have been used: Levenberg–Marquardt (L–M) with a trust-region reflective method [91,92] and Nelder–Mead simplex search method – a direct search method [93] that does not use numerical or analytical gradients. Local minima are commonly reached, especially when the number of variables exceeds two, regardless of the algorithm used, with solutions dependent on the initial guess. In order to overcome this, each minimization problem has been run up to a thousand times the number of variables with different initial points, randomly generated within feasible intervals of the variables. The algorithm is assumed to have found the global minimum when repeated minimizations reach the same solution within a given tolerance. Fig. 2 gives an overview of the number of minimizations required for the various distributions and minimization algorithms, by means of boxplots of the ratio of the number of minimizations to the number of parameters of the distribution. Two-parameter functions are generally fast to fit, some showing a certain preference for a given algorithm (e.g. LGN for L–M and GRA for direct search; WRR and LGL have proved easy to fit with both algorithms tested). TLGL appears to be the easiest-to-fit three-parameter function when using L–M (in general, the faster algorithm for fitting re-scaled functions), but one of the most difficult with direct search. GIL and TGIL are hard to converge to a global minimum, the plain, three-parameter version not being any better than the re-scaled, four-parameter one. Bi-component functions seem to have a slight preference for the direct search method; BiLGN requires similar amount of trials with both algorithms and ExSWE, like most re-scaled functions, is best fitted by L–M.

The efficiency, in terms of R^2, is very close with both algorithms, as Fig. 3 shows: only TLGL shows differences, favoring L–M (which is also the more efficient computationally in this case). For each data set, the fit with a higher R^2 is kept as final (right boxes in Fig. 3).

5. Results and discussion

The determination coefficients in Fig. 3 give a global picture of the quality of the fits. The medians are given in Table 5 (bold, underlined numbers are the higher ones, not mutually different at 0.05 significance). Amongst the two-parameter functions, WRR is the one with higher R^2 (median 0.9886), significantly above GRA's 0.9848 at 0.05 level; GIL has a higher R^2 (0.9894, not different to WRR's to a 0.05 significance), but it has three parameters. Among re-scaled functions, SWE and TWRR are ahead with median R^2 0.9976 and 0.9975 respectively, not mutually different at 0.05 significance; TGRA shows good performance though its median R^2 is lower at 0.05 significance. As might be expected, re-scaled functions outdo their plain versions, since the former encompass one more parameter than the latter. In turn, bi-component functions, generally with two additional parameters, give a much higher R^2, their 25 percentiles always higher than the medians of the re-scaled ones. BiWRR wins with R^2 0.99931 and ExSWE nearly ties with 0.99926; BiGRA's is 0.9990, close to the two above but already statistically different at 0.05 significance. BiGIL, a seven-parameter function, falls behind these.

Besides the determination coefficients, Table 5 gives the median values of $1–R^2$, which represent the fraction of variance unexplained by the fits. The re-scaling reduces this variance by a factor of about four (median ratio) in all functions except GIL, for which the transformation is not effective. The use of bi-components further reduces this unexplained variance by a factor of about two to three except for the GIL, in which this factor is close to five.

Although the determination coefficient is the canonical rating of a fit, it is influenced by the errors in the zone of larger ordinates, while the small ones are neglected; this is relevant when data

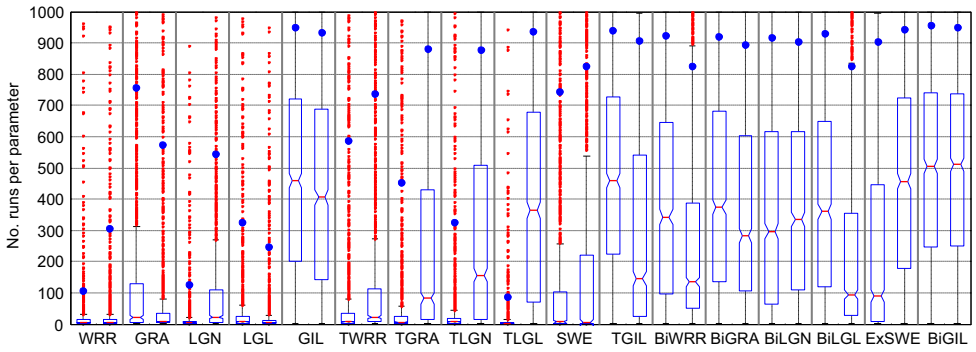

Fig. 2. Number of trials per parameter of the fit. Left boxes: L–M; right boxes: direct search. Blue dots are the 95 percentiles. Whiskers extend up to 1.5 times the interquartile range; beyond that, data are represented as red points. (For interpretation of the references to color in this figure legend, the reader is referred to the web version of this article.)

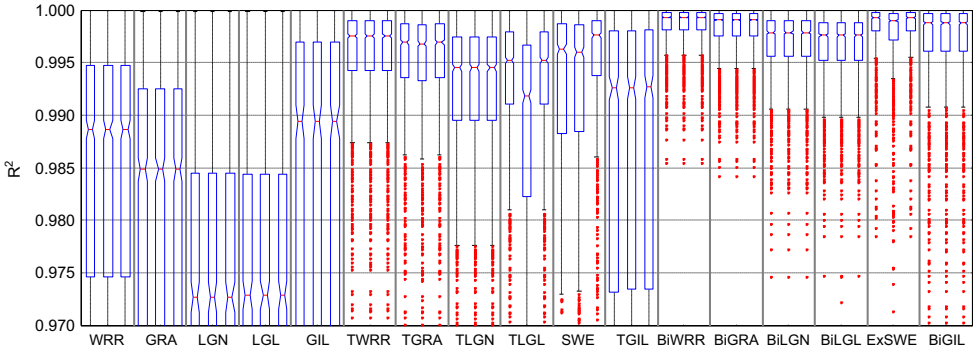

Fig. 3. Determination coefficient. For each distribution, the three boxes are, left: L–M; central: direct search; right: best fit. Whiskers extend up to 1.5 times the interquartile range; beyond that, data are represented as red points. (For interpretation of the references to color in this figure legend, the reader is referred to the web version of this article.)

Table 5
Determination coefficients. Medians.

	R^2			$1-R^2$			Ratio P/T[a]	Ratio T/Bi[b]
	Plain	Re-scaled	Bi-component	Plain	Re-scaled	Bi-component		
WRR	**0.9886**	**0.9975**	**0.9993**	0.0114	0.0025	0.00069	3.72	3.25
GRA	0.9848	0.9969	0.9990	0.0152	0.0031	0.00097	4.19	2.89
LGN	0.9726	0.9945	0.9978	0.0274	0.0055	0.00217	4.05	2.40
LGL	0.9729	0.9952	0.9976	0.0271	0.0048	0.00242	4.65	1.85
SWE	–	**0.9976**	**0.9993**	–	0.0024	0.00074	–	2.29
GIL	**0.9894**	0.9927	0.9988	0.0106	0.0073	0.00124	1.00	4.81

[a] Medians of the ratios of the $1-R^2$ values of the plain function to the re-scaled one.
[b] Medians of the ratios of the $1-R^2$ values of the plain function to the re-scaled one.

spread across a broad range, which is the case in fragment size distributions where data generally spread more than one order of magnitude (see the r_p column in Table 3). R^2 is then a global measure and says nothing about the quality of the fit in the different zones of the data. A convenient form of assessing the behavior of the different functions across the whole range of the data is to calculate the differences between the actual sizes and the ones calculated from the fits at a given passing value; logarithmic differences are used for this purpose:

$$e_L = \log\,(x_p^*/x_p) \tag{12}$$

where (Fig. 4a) x_p is the size at a percent passing p in a given data set and x_p^* the size obtained from a given distribution function F_{CDF} fitted to it:

$$x_p^* = F_{CDF}^{-1}\,(p) \tag{13}$$

Logarithmic errors e_L and relative errors e_r are related as follows:

$$e_r = (x_p^* - x_p)/x_p = x_p^*/x_p - 1 = \exp(e_L) - 1 \tag{14}$$

or

$$e_L = \log\,(e_r + 1) \tag{15}$$

The analysis of errors has been done following the method in [34,35]: the original data are interpolated by piecewise cubic Hermite polynomials in a support of two thousand p values chosen so that their distribution approximately replicates the distribution of passing values from all data sets; the x_p values are the interpolates. This procedure allows the set of passing values used for the error calculations to be the same for all data sets (within the passing domain of each one). Some interpolated curves are shown in Fig. 4b, showing the general characteristics of the Hermite polynomials.

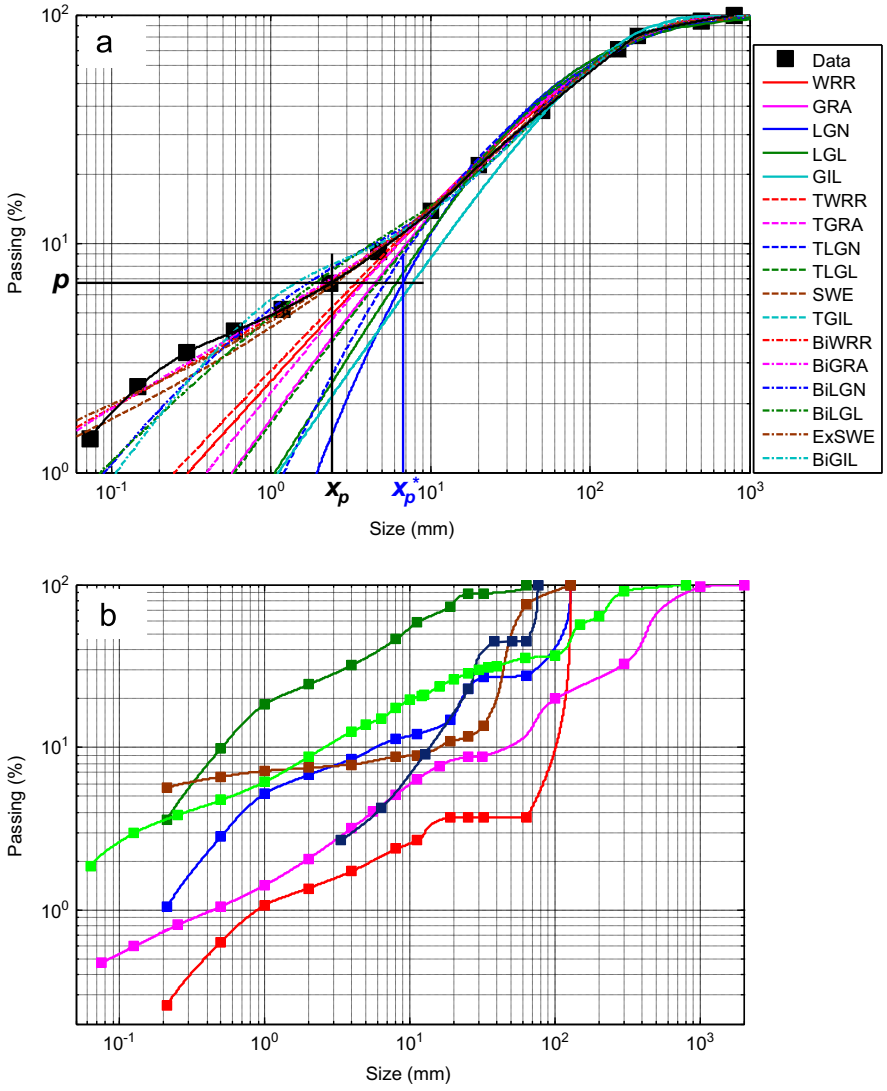

Fig. 4. (a) Fits of distribution functions to a given set; the solid line running through all data points is the interpolated curve for error calculation purposes; and (b) examples of interpolated curves to several data sets.

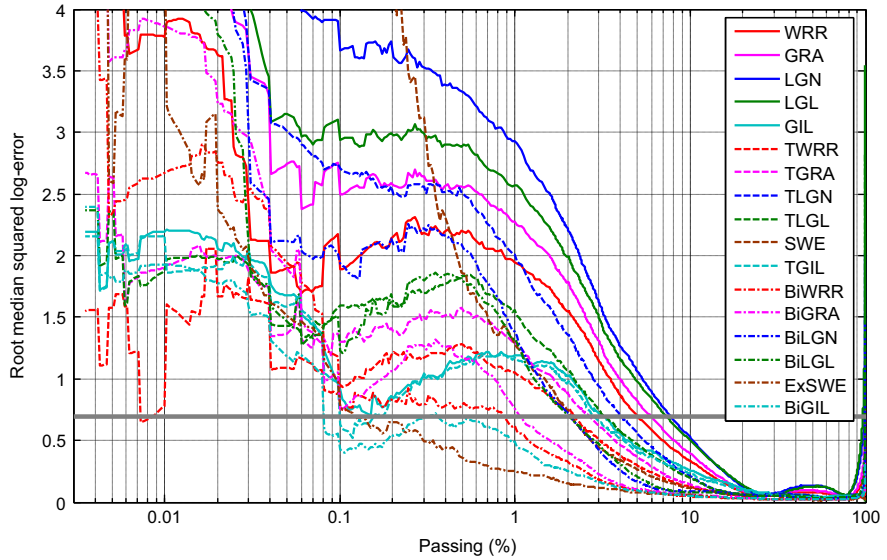

Fig. 5. Log errors in size as function of the percent passing. Curves show the root of the median of squared log errors of all data sets for each passing. The gray horizontal line indicates a log 2 error, which corresponds to a relative error of 100% or −50% (i.e. the calculated value is double or half the data).

Though large differences can be noticed among the different distributions, the pattern of the log errors can be clearly seen in Fig. 5, where the root of the medians of the squared log errors of all data sets at each percent passing are plotted: small errors in the central range (20–80%), increasing towards the upper end (80–100%) and the fines (2–20%), and erratic behavior of errors, with generally wild values below 2%, the very fine range. For each of these zones, the maximum and the mean log-errors are calculated:

$$e_L^{max} = \max\ |e_L(p)|, \quad p_{inf} \le p \le p_{sup} \tag{16}$$

$$e_L^{rms} = \left[\frac{1}{(p_{sup}-p_{inf})}\int_{p_{inf}}^{p_{sup}} e_L^2(p)dp\right]^{1/2} \tag{17}$$

where p_{inf} and p_{sup} are respectively the lower and upper limits of each passing zone (p_{inf} for the very fines is the minimum passing of each data set, and p_{sup} for the coarse is the maximum passing). The integrals in Eq. (17) are calculated numerically by the trapezoidal rule on the support set of p. The medians of e_L^{max} and e_L^{rms} (which can be considered estimators of the expected maximum and average error respectively for each function and passing zone) are plotted in Fig. 6. Table 6 shows the same medians expressed as percent relative errors; the function whose median e_L^{rms} error is lower for each group and passing zone is given first, followed by those not different to it with a 0.05 significance or, in brackets and script type, up to three functions different at a 0.05 significance, in growing order of error. The best three-parameter re-scaled is also listed where there are no such functions amongst the leading ones. Note that sometimes a lower median e_L^{rms} does not correspond with a lower median e_L^{max}.

Table 7 gives the ratios of the e_L^{rms} of each function to the ones of the same type with less parameters: re-scaled to plain, and bi-component to re-scaled; medians of the ratios for each data group are given. Color codes are used to facilitate the reading.

As expected, and predicted by the R^2 analysis, re-scaled functions generally provide a more accurate fit than their plain versions. The exception is TGIL that does not add up any significant advantage to its plain parent; this anomalous behavior may be connected with the fact that the three parameters of this function are all scale factors, so that adding one more (the maximum size is actually another scale factor) does not help to make the function more flexible, and an adjustable shape factor is missing (there are three shape factors in this function: 1, 2 and 3, but they are fixed); actually, the ordinary Gilvarry distribution (GIL) has a worse performance itself than any of the three-parameter functions used. Maximum expected errors for the re-scaled functions (except TGIL) are generally less than about 25% and 10% in the coarse and central ranges respectively, but they grow in the fines up to 100% and more; mean expected errors for the re-scaled are well below 10% in the coarse and central, and between 15% and 40% in the fines. In the very fine range, errors are usually wild for all functions but some bi-components. Group 5 data (laboratory crushing) appears extremely sensitive to the re-scaling transformation in all function types, with large reduction of errors in all ranges and for all functions.

Bi-component distributions are not better than re-scaled ones in the coarse range, probably due to the 100% passing asymptote of the former at infinite size, that is transformed into a tangent at the maximum size in the re-scaled; the ExSWE, a re-scaled function itself without asymptote, improves moderately its single-component (SWE) in this range and is the one with lower errors; BiGIL also improves here its re-scaled version but this only underlines the latter's deficiency. Most of the 3-parameter re-scaled functions are within the best scoring in the coarse range for most of the data types with errors ranging from 8% to 9% in the data group 1 (blasted, mine, which seems to be the most difficult to fit in this zone) to 2% in group five (the easiest to fit). This advantage blurs in the important central range where some bi-component distributions are especially accurate, with mean and maximum errors less than 5% and 10%, respectively; these values

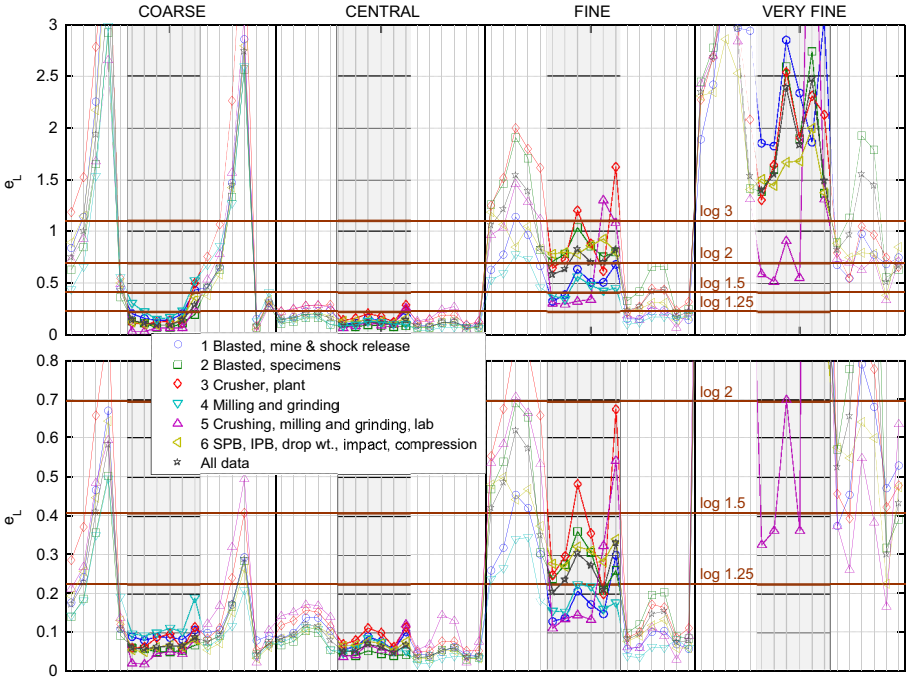

Fig. 6. Log errors in different passing zones. Upper graph: medians of maximum errors for each group of data; lower graph: medians of root mean squared errors. For each zone, the order of the functions from left to right is the same as in Table 1: WRR, GRA, LGN, LGL, GIL, TWRR, TGRA, TLGN, TLGL, SWE, TGIL, BiWRR, BiGRA, BiLGN, BiLGL, ExSWE and BiGIL. The areas of re-scaled functions are shadowed. Horizontal lines are log-errors log 1.25, log 1.50, log 2 and log 3, which correspond to relative errors 25%, 50%, 100% and 200 % respectively.

Table 6
Medians of e_L^{rms} and e_L^{max} as estimators of the mean and maximum errors expected, expressed as relative errors (percent).

Group	Coarse			Central			Fine			Very fine		
1	ExSWE	8	17	BiGIL	4	8	BiWRR	6	16	BiWRR	45	96
	TGRA	8	18	BiGRA	4	8	BiGIL	6	15	BiGRA	57	72
	SWE	9	23	ExSWE	4	9	BiGRA	6	16	ExSWE	60	97
	TLGL	9	15	BiWRR	4	10	ExSWE	7	19	BiGIL	70	112
	TLGN	9	15									
	BiGIL	9	36									
	TWRR	9	23									
				SWE	6	12	TWRR	14	39	SWE	234	544
2	ExSWE	4	8	ExSWE	3	6	BiGIL	9	27	ExSWE	37	74
	[*TLGL*]	5	7	[*BiWRR*]	3	7	ExSWE	9	23	BiGIL	47	87
	[*TLGN*]	5	7	[*BiGIL*]	3	7	BiWRR	10	39	[*BiWRR*]	77	143
				SWE	4	8	SWE	23	113	TWRR	174	300
3	ExSWE	5	9	BiWRR	5	12	ExSWE	9	26	BiGRA	48	73
	SWE	6	12	ExSWE	5	10	BiWRR	9	24	ExSWE	52	112
	TWRR	6	12	BiGIL	5	13	BiGRA	10	31	BiWRR	58	120
	TGRA	6	11	BiGRA	5	15	BiGIL	12	37	BiGIL	61	93
	BiGIL	7	38							BiLGL	117	163
										BiLGN	133	184
				SWE	6	14	SWE	22	85	TWRR	192	269
4	ExSWE	4	13	BiWRR	2	4	BiGRA	3	12	Few data		
	[*BiWRR*]	6	97	BiGRA	2	4	BiWRR	4	10			
	[*BiGIL*]	7	50	[*BiGIL*]	3	6	[*BiLGL*]	6	18			
	TGRA	10	25	TWRR	5	9	TGRA	17	41			
5	TGRA	2	3	ExSWE	2	5	ExSWE	3	7	ExSWE	18	39
	ExSWE	2	3	[*TWRR*]	4	7	[*BiGRA*]	6	15	[*BiGRA*]	30	101
	TWRR	2	3	[*TGRA*]	4	9	[*BiWRR*]	6	20	[*TWRR*]	39	80
							TWRR	12	36			
6	ExSWE	3	5	BiWRR	3	7	ExSWE	6	16	ExSWE	25	46
	[*TGRA*]	5	11	BiGRA	3	7	BiGIL	6	19	[*BiGIL*]	60	133
	[*BiWRR*]	5	46	ExSWE	3	6	[*BiWRR*]	8	25	[*BiGRA*]	73	111
				BiGIL	3	7						
				SWE	5	12	TGRA	31	123	TWRR	174	352
All data	ExSWE	4	8	ExSWE	3	7	ExSWE	8	18	ExSWE	35	67
	[*TGRA*]	6	12	[*BiWRR*]	3	8	BiGIL	8	25	[*BiGIL*]	54	94
	[*TWRR*]	6	15	[*BiGIL*]	4	8	BiWRR	8	26	[*BiWRR*]	69	127
				SWE	5	10	TWRR	23	79	TWRR	171	302

Errors in this table are given, for quick interpretation, in relative form. They are derived from root mean squared or from absolute log-errors, all positive, but the negative counterpart is implicit. Unlike logarithmic error, relative error is not symmetric with respect to zero: log-errors $\pm$ log 2 (calculated value double or half the data) correspond to relative errors +100% and −50%. The values in the table are the positive ones.
For each group and passing zone the distributions whose median e_L^{rms} are not different at 0.05 significance are listed in regular font; in script between brackets, functions immediately following the lower error one whose error is significantly different. The best 3-parameter re-scaled one is reported below them where there are no such functions amongst the best ones.

are, however, not much lower than those of some re-scaled functions; SWE, TWRR and TGRA are generally a good option in the central range if the extra effort to fit a five-parameter function is considered. In group 5, TWRR and TGRA are second to the ExSWE even in the central range. The likely reason for this excellent behavior of re-scaled functions is that group 5 is the least right-skewed group (in fact, more than half of it is moderately left-skewed); the short right tail makes them well suited for re-scaled, right-limited functions and not for plain, right-infinite ones. High kurtosis is usually connected with some bi-modality and group 5 has the lower kurtosis of all groups so there is generally no gain in fitting bi-components (bi-modals) to them. This does not hold for the ExSWE, whose re-scaled nature allows it to fit group 5 data extremely well in all ranges.

The benefits of the bi-component functions are apparent in the fine range where errors (maximum and mean generally less than 30% and 10% respectively for the best ones) are often less than half the re-scaled ones. Also in the very fines, mean errors are moderate for some bi-component functions (50% can be expected in the best case for some data groups) though maximum errors can be very high (often in excess of 100%, even in the best cases); ExSWE is clearly the best one in this range, followed by BiGIL (note that this is a seven-parameter function) and BiWRR; ExSWE is actually among the best-fitting in nearly all groups and ranges. Other bi-component functions scoring high are BiGIL, BiWRR and, to a lesser degree, BiGRA. BiLGN and BiLGL show mediocre results, with errors systematically higher than the rest of their type.

Table 8 summarizes the errors for the different ranges; expected errors are medians of e_L^{rms} and maximum errors are medians of e_L^{max}.

How much into the fines can the re-scaled functions be reasonably used may be decided from Fig. 7, which shows the maximum errors (medians of all data sets, in relative form) for the re-scaled and bi-component distributions, as a function of the percent passing. The best re-scaled functions, SWE, TWRR and TGRA have an expected maximum error less than 15% at 10% passing, whereas at 20% passing, expected maximum are a mere 6%. Below 10% passing, maximum expected errors increase rapidly: at 8% passing they are about 15% (SWE) to 20% (TGRA) and at 5% passing they are about 30% (SWE) to 45% (TGRA): the use of bi-components should be seriously considered.

Besides the type of the data, the best fitting functions have been analyzed against the descriptive statistics used in Section 3: coefficient of variation, log-slope, log-p range, log-x range, skewness and excess kurtosis. Fig. 8 shows box plots (with only the interquartile range and the median shown) of the statistics of the data sets best fitted by a given distribution in each passing zone. Only distributions that are the best-fitting (i.e. lower e_L^{rms}) in the range of interest for more than 4% of all data sets have been considered; medians of the descriptors of all sets with data in the

Table 7
Ratio (medians) of e_L^{rms} of the plain to the re-scaled, and of the bi-component to the re-scaled functions.

		PLAIN/RE-SCALED				RE-SCALED/BI-COMPONENT			
		CO	CE	FI	VF	CO	CE	FI	VF
WRR	Group 1	1.8	1.2	1.7	1.4	0.9	1.5	2.3	2.8
	Group 2	2.6	1.5	1.9	1.8	0.8	1.3	2.2	1.6
	Group 3	4.0	1.4	2.2	1.8	0.8	1.6	2.4	1.8
	Group 4	1.1	1.3	1.5	-	1.7	2.5	3.6	-
	Group 5	9.6	3.8	5.3	4.7	0.2	0.5	1.7	0.7
	Group 6	3.0	1.2	1.6	1.5	1.1	2.3	3.6	2.0
	All	2.7	1.4	1.8	1.8	0.9	1.5	2.6	1.7
GRA	Group 1	2.8	1.3	1.9	1.4	0.7	1.5	2.1	3.6
	Group 2	3.7	1.7	1.9	1.7	0.7	1.3	2.3	1.5
	Group 3	4.6	1.4	2.0	1.7	0.6	1.6	2.6	2.7
	Group 4	1.6	1.3	1.5	-	1.0	2.6	5.5	-
	Group 5	17.6	3.1	4.2	5.1	0.1	0.5	1.4	0.6
	Group 6	4.0	1.3	1.6	1.6	0.8	2.2	3.3	2.0
	All	3.8	1.5	1.9	1.7	0.7	1.5	2.6	1.6
LGN	Group 1	5.5	1.5	1.8	1.3	0.5	1.6	2.7	2.7
	Group 2	6.7	1.7	1.7	1.4	0.3	1.1	2.0	1.3
	Group 3	7.0	1.4	1.7	1.4	0.4	1.4	2.4	2.4
	Group 4	3.5	1.2	1.6	-	0.7	2.4	3.8	-
	Group 5	14.5	2.5	3.9	2.8	0.1	0.4	1.1	0.7
	Group 6	7.9	1.4	1.6	1.3	0.4	1.7	2.5	1.9
	All	6.8	1.6	1.7	1.4	0.4	1.3	2.3	1.4
LGL	Group 1	7.3	1.6	2.0	1.5	0.3	1.3	2.0	2.2
	Group 2	9.6	1.9	1.8	1.6	0.2	0.9	1.6	1.1
	Group 3	8.9	1.5	1.8	1.6	0.2	1.3	2.3	1.9
	Group 4	4.6	1.3	1.6	-	0.4	2.0	3.6	-
	Group 5	18.7	3.1	4.0	5.0	0.1	0.3	1.1	0.6
	Group 6	10.2	1.5	1.7	1.5	0.3	1.5	2.6	1.9
	All	9.5	1.8	1.8	1.6	0.2	1.2	2.0	1.2
SWE	Group 1	-	-	-	-	1.0	1.1	1.7	2.4
	Group 2	-	-	-	-	1.0	1.1	1.8	4.4
	Group 3	-	-	-	-	1.0	1.1	1.5	2.4
	Group 4	-	-	-	-	1.3	1.1	1.9	-
	Group 5	-	-	-	-	1.6	2.2	12.0	25.6
	Group 6	-	-	-	-	1.5	1.5	4.7	5.8
	All	-	-	-	-	1.0	1.2	2.2	4.5
GIL	Group 1	1.0	1.0	1.0	1.0	1.5	2.3	4.6	2.6
	Group 2	1.0	1.0	1.0	1.0	1.0	1.4	2.8	1.5
	Group 3	1.0	1.0	1.0	1.0	1.8	2.2	6.1	2.7
	Group 4	1.0	1.0	1.0	-	2.4	2.5	6.3	-
	Group 5	1.0	1.0	1.0	1.0	0.9	1.5	5.6	3.1
	Group 6	1.0	1.0	1.0	1.0	1.7	2.9	5.9	1.7
	All	1.0	1.0	1.0	1.0	1.2	1.8	4.3	1.9

Notes:
- Blank boxes correspond to Group 4 in the very fines region which only has three sets with data, and to the plain/re-scaled comparison for the Swebrec, not applicable.
- Colors apply to the intervals: ∞-5-2-1.05 (greenish), 1.05-0.95 (grey), and 0.95-0.5-0.2-0 (reddish); more intense away from 1.

Table 8
Summary of errors; expected and maximum are medians of e_L^{rms} and e_L^{max} for all data sets; expressed as relative errors (%).

Range	Functions	No. of param.	Expected error (%)	Maximum error (%)
Coarse (100–80%)	ExSWE	5	4	8
	All 3-p re-scaled: TGRA, TWRR, TLGN, SWE, TLGL	3	6–7	10–15
	BiGIL	7	7	35
	BiWRR, BiGRA	5	7–9	58–92
	TGIL	4	9	34
	GIL	3	11	53
	WRR	2	18	111
	BiLGN	5	19	320
Central (80–20%)	ExSWE	5	3	7
	BiWRR, BiGRA	5	3–4	8
	BiGIL	7	4	8
	All 3-p re-scaled: SWE, TWRR, TGRA, TLGL, TLGN	3	5–7	10–15

Table 8 (*continued*)

Range	Functions	No. of param.	Expected error (%)	Maximum error (%)
	TGIL	4	7	15
	BiLGN, BiLGL	5	6	12–13
	GIL	3	8	17
	WRR	2	8	15
Fine (20–2%)	ExSWE, BiWRR	5	8	18–26
	BiGIL	7	8	25
	Other 5-p bi-components: BiGRA, BiLGN, BiLGL	5	10–16	31–54
	TWRR, SWE, TGRA	3	23–26	79–101
	Other 3-p re-scaled: TLGL, TLGN	5	31–36	102–129
	TGIL	4	39	128
	GIL	3	42	132
	WRR	2	52	187
Very fine ($<2\%$)	ExSWE	5	35	67
	BiGIL	7	54	94
	BiWRR, BiGRA	5	69–93	127–163
	TWRR	3	171	302
	BiLGL, BiLGN	5	189–198	321–370
	TGIL	4	219	342
	TGRA	3	227	370

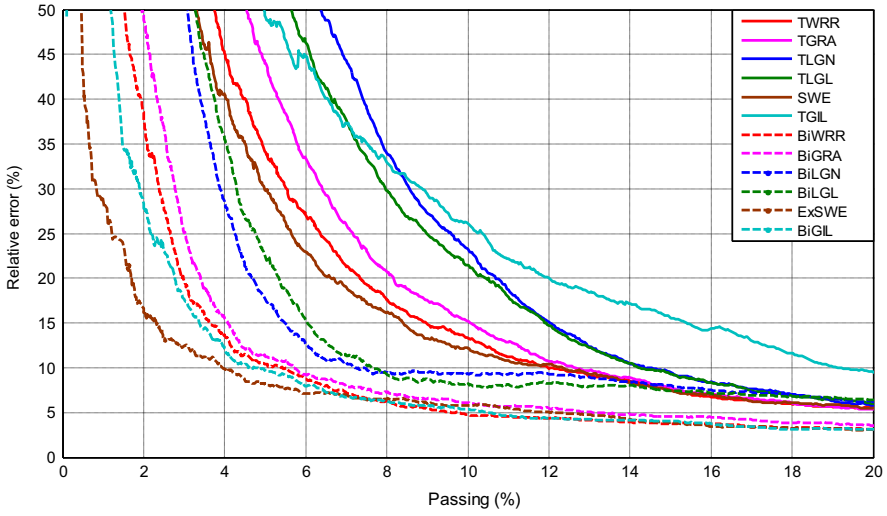

Fig. 7. Local maximum errors at each percent passing. Medians of all data sets.

passing range concerned are also plotted (horizontal lines) for reference. Solid bars are used for distributions scoring as best-fitting in more than 10% of the data sets.

The upper two charts in Fig. 8 analyze the dispersion; generally speaking, data sets where re-scaled distributions are strong have low dispersion (except in the coarse range for TWRR) while bi-component ones are more inclined towards higher dispersions. It must be noted that the best functions' bars (those scoring more than 10% winners) are generally centered with the global median, which means that they do well in high and low dispersion data. This also applies to other indicators.

There are no noticeable trends in the x and p log ranges of the sets best fitted by the various distributions; long size ranges appear to be preferred by BiWRR with good scores in all ranges; BiGIL has a similar result in the coarse range.

The good behavior of the re-scaled functions in the coarse range is associated with data sets of lower skewness as was observed with the group 5 anomaly; this is natural since long right tails (encompassing higher skewness) are cut by the re-scaling. Even the ExSWE (a re-scaled function), the best fitting function in most cases, has some tendency to work better at relatively low skewness while all other bi-component functions do better in higher skewness.

Kurtosis does not add much to the analysis as it replicates the trends of the skewness, to which it is related in skewed distributions. High kurtosis may be a sign of bi-modality; in this sense, a certain preference of some bi-component functions (bimodal GRA, LGN, LGL) is only natural.

6. Conclusions

A large-scale assessment of 17 distributions to represent fragmented rock sizes has been carried out; the distributions are Weibull (WRR), Grady (GRA), log-normal (LGN), log-logistic (LGL) and Gilvarry (GIL), in their regular, re-scaled, and bi-component forms; together with them, the Swebrec distribution (SWE) and its bi-component extension (ExSWE) complete the suite; the fragmentation data base comprises 1234 sets obtained entirely by sieving. The results provide guidelines for deciding what

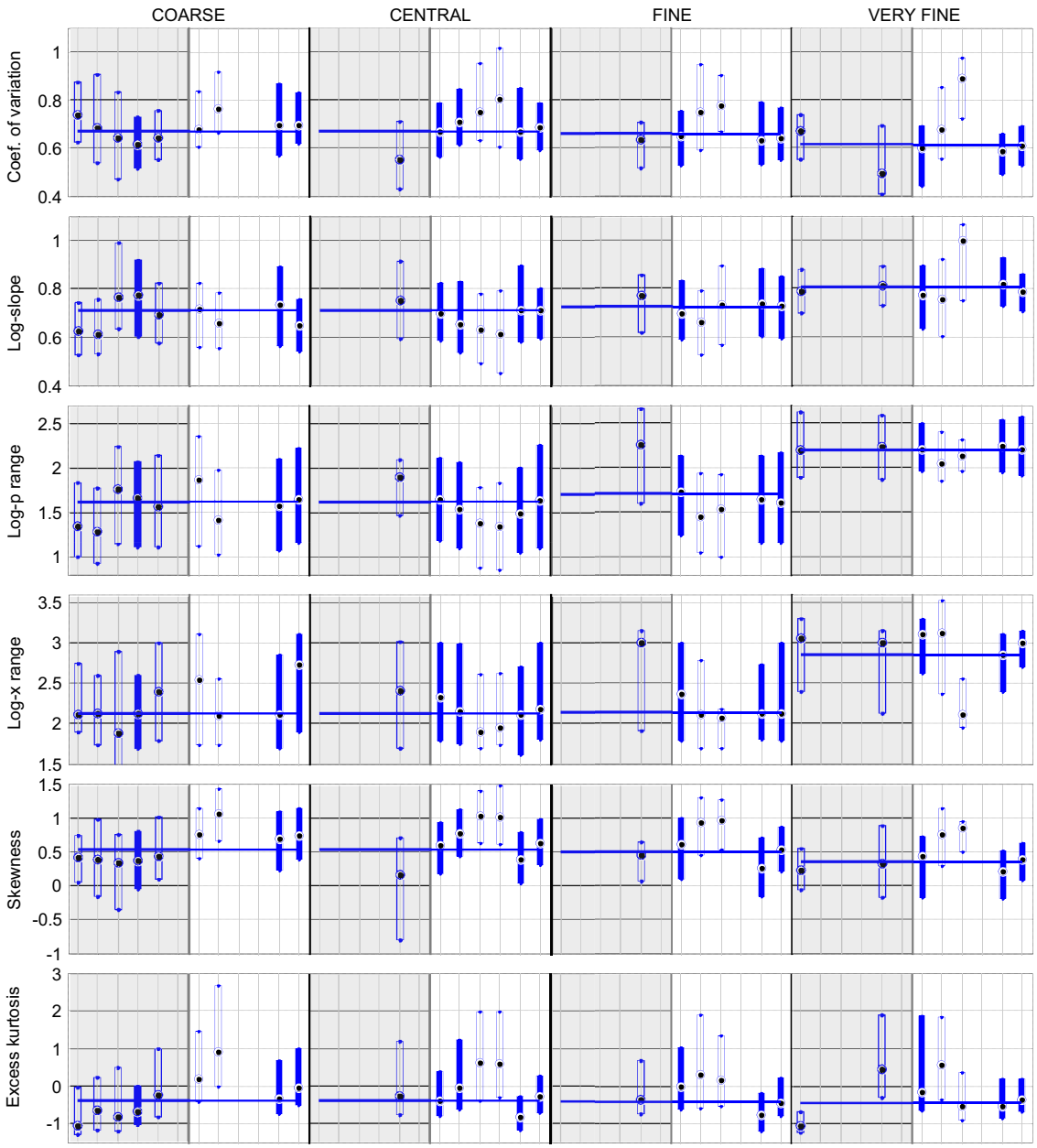

Fig. 8. Descriptive statistics of the data sets that are best fitted by each of the distributions. Only re-scaled and bi-components are shown. Bars show the interquartile range of the statistics of the data sets best fitted by each distribution. The position of the distributions are, from left to right in each range: TWRR, TGRA, TLGN, TLGL, SWE, TGIL, BiWRR, BiGRA, BiLGN, BiLGL, ExSWE, BiGIL; the areas corresponding to re-scaled functions are shadowed. Horizontal lines are the medians of the statistics of all the sets with data in the range concerned.

distribution function to use (and what not to use) for describing rock fragment size with reasonable accuracy within the range of interest.

In terms of determination coefficient, WRR is the best two-parameter distribution for describing rock fragments; the median R^2 of the 1234 data sets fitted is 0.9886. Among re-scaled, three-parameter distributions, SWE and TWRR are ahead with median R^2 0.9976 and 0.9975 respectively. Five-parameter BiWRR and ExSWE tie in the top with median R^2 0.9993. In terms of unexplained variance ($1–R^2$), the results show that re-scaling generally reduces it by a factor of about four and that bi-component distributions further reduce this unexplained variance in most cases by a factor of about two to three.

Errors in calculating sizes have been used to assess the performance distributions in the different passing zones: coarse, central, fine and very fine, arbitrarily defined by the limits 100–80–20–2–0% passing. Errors are limited in the central range, and increase towards the coarse and fine ends.

The ordinary WRR (despite being the best two-parameter function), can only be used, with expected errors of about 8% in the calculation of sizes, in the central range (20–80% passing). Expected errors increase away from that range to 18% in the coarse ($>$ 80% passing) and 52% in the fines (20–2% passing).

Bi-component are not better than re-scaled functions in the coarse range for most of the data types; this does not apply to ExSWE, a re-scaled function itself. Three-parameter re-scaled distributions perform very well also in the central range, with errors not much higher than the best bi-components (ExSWE, BiWRR and BiGRA) and, in some cases, lower than their bi-component (BiLGL and BiLGN). TWRR, TGRA and SWE are

generally the best re-scaled functions in all types of material; these may still be used if errors of about 25% can be accepted in the fines, though maximum errors may exceed 100%.

The benefits of the bi-components are apparent in the fine range, where expected and maximum errors are often less than half the re-scaled ones. Also in the very fines, errors are moderate for some bi-components (ExSWE and, to a lesser extent, BiWRR and BiGRA), though maximum errors can be very high.

ExSWE is the best fitting function in general, in nearly all groups of data and across the whole passing range. BiWRR and BiGRA follow (except for the coarse range, where re-scaled functions are preferable). BiLGN and BiLGL are generally the worse bi-component functions. Except in the coarse range, BiGIL often pairs with ExSWE as best fit though, being a seven-parameter function, there are no reasons for using it in place of some of the best five-parameter ones.

No general quantitative indications can be given on what characteristics a data set must have to be best fitted by one or another distribution; however, bi-components are more appropriate for data with higher dispersions. The good behavior of the three-parameter, re-scaled functions in the coarse range is associated with data sets of lower skewness and kurtosis while there is a certain preference of some bi-components (BiGRA, BiLGN, BiLGL) at higher skewness and kurtosis.

Since fitting a five-parameter function is significantly more difficult than fitting a three-parameter one, as the likeliness of local solutions in the minimization problem increases with the number of parameters, re-scaled distributions are the best choice down to about 20% passing. If the interest lies in finer material, some re-scaled distributions (TWRR, SWE and TGRA) may still be used down to about 8–10% passing but serious consideration should be given to the bi-components, especially ExSWE, BiWRR and BiGRA. These become imperative if the data extend further down to lower percent passing.

Acknowledgments

We wish to thank all those that have generously provided fragment size data. Special thanks to Sushil Bhandari, Claude Cunningham, Daniel Johansson and Cameron McKenzie.

References

[1] Cunningham CVB. The Kuz–Ram model for prediction of fragmentation from blasting. In: Proceedings of the 1st international symposium on rock fragmentation by blasting, Luleå, Sweden, 22–26 August 1983; 1983. p. 439–52.
[2] Cunningham CVB. Fragmentation estimations and the Kuz–Ram model – four years on. In: Proceedings of the 2nd international symposium on rock fragmentation by blasting, Keystone, CO, USA, 23–26 August 1987; 1987. p. 475–87.
[3] Ouchterlony F, Niklasson B, Abrahamsson S. Fragmentation monitoring of production blasts at MRICA. In: Proceedings of the 3rd international symposium on rock fragmentation by blasting, Brisbane, Australia, 26–31 August 1990. p. 283–9.
[4] Otterness RE, Stagg MS, Rholl SA, Smith NS. Correlation of shot design parameters to fragmentation. In: Proceedings of the 7th annual symposium on explosives and blasting research, Las Vegas, NV, USA, 6–7 February 1991. p. 179–90.
[5] Kou S, Rustan A. Computerized design and result prediction of bench blasting. In: Rossmanith HP, editor. Proceedings of the 4th international symposium on rock fragmentation by blasting (FRAGBLAST 4), Vienna, 5–8 July 1993. p. 263–71.
[6] Djordjevic N. Two-component model of blast fragmentation. In: Proceedings of the 6th international symposium on rock fragmentation by blasting, Johannesburg, South Africa, 8–12 August 1999. p. 213–9.
[7] Kanchibotla SS, Valery W, Morrell S. Modelling fines in blast fragmentation and its impact on crushing and grinding. In: Proceedings of Explo'99 – a conference on rock breaking, Kalgoorlie, Australia, 7–11 November 1999. p. 137–44.
[8] Chung SH, Katsabanis PD. Fragmentation prediction using improved engineering formulae. Int J Blasting Fragm 2000;4(3–4):198–207.
[9] Thornton DM, Kanchibotla SS, Esterle JS. A fragmentation model to estimate ROM size distribution of soft rock types. In: Proceedings of the 27th annual conference on explosives and blasting technique, Orlando, FL, 28–31 January 2001. p. 41–53.
[10] Lynch AJ, editor. Mineral crushing and grinding circuits – their simulation, optimisation, design and control. Developments in mineral processing. New York: Elsevier Scientific Publishing; 1977.
[11] Karra VK. Development of a model for predicting the screening performance of a vibrating screen. CIM Bull 1979;72(804):167–71.
[12] Napier-Munn TJ, Lynch AJ. The modelling and computer simulation of mineral treatment processes – current status and future trends. Miner Eng 1992;5 (2):143–67.
[13] Napier-Munn TJ, Morrell S, Morrison RD, Kojovic T. Mineral comminution circuits: their operation and optimisation. JKMRC monograph series in mining and mineral processing. Brisbane, QLD: The University of Queensland; 1996.
[14] Marlin TE, editor. Process control – designing processes and control systems for dynamic performance. New York: McGraw-Hill; 2000.
[15] King RP. Modeling and simulation of mineral processing systems. Oxford: Butterworth-Heinemann; 2001.
[16] Fuerstenau MC, Han KN. Principles of mineral processing. Littleton, CO: Society for Mining, Metallurgy and Exploration; 2003.
[17] Liu Y, Spencer S. Dynamic simulation of grinding circuits. Miner Eng 2004;17 (11–12):1189–98.
[18] Smith H. Process simulation and modelling. In: Mike DA, Wills BA, editors. Developments in mineral processing, vol. 15. Advances in gold ore processing. Philadelphia, PA: Elsevier; 2005. p. 109–21.
[19] Wills BA, Napier-Munn TJ. Mineral processing technology: An introduction to the practical aspects of ore treatment and mineral recovery. London: Elsevier; 2006.
[20] Gupta A, Yan DS. Mineral processing design and operations. Amsterdam: Elsevier; 2006.
[21] Rosin P, Rammler E. The laws governing the fineness of powdered coal. J Inst Fuel 1933;7:29–36.
[22] Weibull W. A statistical theory of the strength of materials. Ingeniörsvetenskapsakademiens Handlingar 1939;151:1–45.
[23] Weibull W. A statistical distribution function of wide applicability. J Appl Mech ASME 1951;18:293–7.
[24] Ouchterlony F. The Swebrec© function, linking fragmentation by blasting and crushing. Min Tech (Trans Inst Min Metal A) 2005;114:A29–44.
[25] Ouchterlony F. What does the fragment size distribution of blasted rock look like? In: Holmberg R, editor. Proceedings of the 3rd world conference on explosives and blasting, Brighton, 13–16 September 2005. p. 189–99.
[26] Blair DP. Curve-fitting schemes for fragmentation data. Int J Blasting Fragm 2004;8(3):137–50.
[27] Grady DE, Kipp ME. Geometric statistics and dynamic fragmentation. J Appl Phys 1985;58(3):1210–22.
[28] Grady DE. Particle size statistics in dynamic fragmentation. J Appl Phys 1990;68(12):6099–105.
[29] Gilvarry JJ. Fracture of brittle solids. I. Distribution function for fragment size in single fracture (theoretical). J Appl Phys 1961;32(3):391–9.
[30] Gilvarry JJ, Bergstrom BH. Fracture of brittle solids. II. Distribution function for fragment size in single fracture (experimental). J Appl Phys 1961;32 (3):400–10.
[31] Sil'vestrov VV. Fragmentation of a steel sphere under a high-velocity impact on a highly porous thin bumper. Combust Expl Shock Waves 2004;40 (2):238–52.
[32] Sil'vestrov VV. Application of the Gilvarry distribution to the statistical description of fragmentation of solids under dynamic loading. Combust Explos Shock Waves 2004;40(2):225–37.
[33] Sanchidrián JA, Ouchterlony F, Segarra P, Moser P, López LM. Evaluation of some distribution functions for describing rock fragmentation data. In: Sanchidrián JA, editor. Proceedings of the 9th international symposium on Rock Fragmentation by Blasting (FRAGBLAST 9), Granada, Spain, 13–17 September 2009. Leiden: CRC Press/Balkema; 2010. p. 239–48.
[34] Sanchidrián JA, Ouchterlony F, Moser P, Segarra P, López LM. Performance of some distributions to describe rock fragmentation data. Int J Rock Mech Min Sci 2012;53:18–31.
[35] Sanchidrián JA, Segarra P, López LM, Ouchterlony F, Moser P. On the performance of truncated distributions to describe rock fragmentation. In: Sanchidrián JA, Singh AK, editors. Measurement and analysis of blast fragmentation, New Delhi, India, 24–25 November 2012. London: Taylor and Francis; 2013. p. 87–96.
[36] Sanchidrián JA, Segarra P, López LM. A practical procedure for the measurement of fragmentation by blasting by image analysis. Rock Mech Rock Eng 2006;39(4):359–82.
[37] Bond FC, Whitney BB. The work index in blasting. In: Proceedings of the 3rd US symposium on rock mechanics, Golden, CO. Q Colo School Mines 1959;54 (3):77–82.
[38] McKenzie C. 2003, personal communication.
[39] Olsson M, Bergqvist I. Fragmentation in quarries. In: Proceedings of the discussion meeting BK 2002. Stockholm, Sweden: Swedish Rock Construction Committee; 2002. p. 33–8 [in Swedish].
[40] Gynnemo M. Investigation of governing factors in bench blasting. Full-scale tests at Kållered and Billingsryd. Publ. A84. Gothenburg, Sweden: Chalmers University, Department of Geology; 1997 [in Swedish].
[41] Cunningham CVB. 2003, Personal communication.

[42] Ash RL. The influence of geological discontinuities on rock blasting. (Ph.D. thesis). Minneapolis: University of Minnesota; 1973; 289.
[43] Bailing M, Shiqi Z, Dingxiang Z, Chuji G. A study of bench blasting in rhyoporphyry at a reduced scale and the statistical analysis of the regularity for fragmentation distribution. In: Proceedings of the first international symposium on rock fragmentation by blasting, Luleå, Sweden, 1983. p. 857–72.
[44] Lundberg S, Fagervall U. Tappning, transport och krossning av skivrasberg på 320 m avv. i KUJ. Delutredning 1: Siktanalys av skivrasberg and Delutredning 2: Siktanalys av ortberg. (Internal report 116-1071). LKAB; 1961 ([in Swedish]).
[45] Maripuu R. Undersökning av siktanalys och styckeform hos representativt styckefall från skivrasbrytningen vid LKAB, Kiruna. (Degree thesis). Luleå Unieversity of Technology; 1968 ([in Swedish]).
[46] Stagg MS, Nutting MJ. Influence of blast delay time on rock fragmentation: one- tenth-scale tests. US Bureau of Mines IC 9135. Minneapolis, MN: USBM; 1987; 79–95.
[47] Wimmer M, Kangas J, Ouchterlony F. The fragment size distribution of Kiruna magnetite loaded from a draw point - evaluation and analysis of a full-scale test. Report 2008:U2. Stockholm: Swebrec – Swedish Blasting Research Centre; 2008.
[48] Wimmer M, Ouchterlony F, Moser P. The fragment size distribution of Kiruna magnetite, from model-scale to run of the mine. In: Proceedings of the 5th international conference and exhibition on mass mining, Luleå, Sweden 9–11 June 2008.
[49] Fourie FJ, Zaniewski T. Fragmentation studies and improvement in the MCF at Kopanang Mine. In: Proceedings of the 8th international symposium on Rock Fragmentation by Blasting (FRAGBLAST 8), Santiago, Chile, 7–11 May 2006. p. 350–64.
[50] Grimshaw HC. The fragmentation produced by explosive detonated in stone blocks. In: Walton WH, editor. Mechanical properties of non-metallic brittle materials. Proceedings of the conference on non-metallic brittle materials, London, April 1958. London: Butterworth; p. 380–8.
[51] Moser P, Grasedieck A, Arsic V, Reichholf G. Charakteristik der Korngrössenverteilung von Sprenghauwerk im Feinbereich. Berg- Hüttenmänn Monatshefte 2003;148:205–16 (in German).
[52] Moser P, Grasedieck A, du Mouza J, Hamdi E. Breakage energy in rock blasting. In: Holmberg R, editor. Proceedings of the 2nd world conference on explosives and blasting, Prague, 10–12 September. Rotterdam: Balkema; 2003. p. 323–34.
[53] Moser P, Grasedieck A, Olsson M, Ouchterlony F. Comparison of the blast fragmentation from lab-scale and full-scale tests at Bårarp. In: Holmberg R, editor. Proceedings of the 2nd world conference on explosives and blasting, Prague, 10–12 September 2003. Rotterdam: Balkema; 2003. p. 449–58.
[54] Kristiansen J. Blastability of rock, small-scale tests in rock blocks. Report 548095-4. Oslo: Norwegian Geotechnical Institute; 1994 (in Norwegian).
[55] Kristiansen J. Blastability of rock, full-scale blasting tests with different hole diameters. Report 548095-5. Oslo: Norwegian Geotechnical Institute; 1995 (in Norwegian).
[56] Rustan A, Naarttijärvi T. The influence from specific charge and geometric scale on fragmentation. Report FG8322. Luleå, Sweden: Swedish Mining Research Foundation; 1983.
[57] Svahn V. Generation of fines around a borehole: a laboratory study. Proceedings of the 7th international symposium on rock fragmentation by blasting, Beijing, 11–15 August 2002. Beijing: Metallurgical Industry Press; 2002; 122–127.
[58] Svahn V. Generation of fines in bench blasting. (Licenciate thesis, Pub. A104). Gothenburg, Sweden: Department of Geology, Chalmers University; 2003.
[59] Badal R. Rock blasting with discontinuities. New Delhi: International Book Traders and Publishers; 1995.
[60] Bhandari S. Studies on rock fragmentation in blasting. (Ph.D. thesis). Sydney: University of New South Wales; 1975.
[61] Nie SL. New hard rock fragmentation formulas based on model and full-scale tests. (Licenciate thesis). University of Luleå; 1988.
[62] Johansson D. Fragmentation and waste rock compaction in small-scale confined blasting. (Licentiate thesis 2008:30). Luleå: Luleå University of Technology; 2008.
[63] Johansson D, Ouchterlony F. Shock wave interactions in rock blasting: the use of short delays to improve fragmentation in model-scale. Rock Mech Rock Eng 2013;46:1–18.
[64] Hänninger A, Larsson L, Slokenbergs M. Investigation of results and capacities when crushing andesite. (Diploma thesis no. 308). Hydraulics Laboratory Stockholm: Royal Institute of Technology; 1988 (in Swedish).
[65] Moser P. Less fines production in aggregate and industrial minerals industry. In: Holmberg R, editor. Proceedings of the 2nd world conference on explosives and blasting, Prague, 10–12 September 2003. Rotterdam: Balkema; 2003. p. 335–43.
[66] Kristiansen J. A study of how the velocity of detonation affects fragmentation and the quality of fragments in a muckpile. In: Proceedings of Explo'95. Publication series no. 6/95. Carlton, Vic., Australia: AusIMM; 1995. p. 437–44.
[67] Boliden. Bandprov. Technical report TM-REP2003/45; 2003.
[68] Chi G. A study of comminution efficiency in relation to controlled blasting in mining. (Ph.D. thesis). Reno: University of Nevada; 1994.
[69] Chi G, Fuerstenau MC, Bradt RC, Ghosh A. Improved comminution efficiency through controlled blasting during mining. Int J Mineral Proc 1996;47:93–101.
[70] Fuerstenau MC, Chi G, Bradt RC, Ghosh A. Increased ore grindability and plant throughput with controlled blasting. Min Eng 1997;49(12):70–5.
[71] Adolfsson G. LKAB process technology Kiruna; 2008. Personal communication.
[72] Hahne R, Pålsson BI, Samskog PO. Ore characterisation for – and simulation of –primary autogenous grinding. Miner Eng 2003;16:13–9.
[73] Lin CL, Yen YK, Miller JD. Plant-site evaluations of the OPSA system for on-line particle-size measurement from moving belt conveyors. Miner Eng 2000;13 (8–9):897–909.
[74] Leoben MU. The natural breakage characteristics (NBC) and energy register functions for the rock mass of the quarries Nordkalk, Cementos Portland and Hengl Bitustein. Less fines, EU Project GRD-2000-25224. Technical report 33; 2002.
[75] Rohrmoser S, Hollerer H, Comoli C. Magnetite ore samples from LKAB´s operation in Kiruna/Sweden: optimized comminution sequence, natural breakage characteristic and energy register. Report 2007:U1. Stockholm: Swebrec – Swedish Blasting research Centre; 2007.
[76] Donovan JG. Fracture toughness based models for the prediction of power consumption, product size, and capacity of jaw crushers. (Ph.D. thesis). Blacksburg, VA: Virginia Polytechnic Institute and State University; 2003.
[77] Moosavi-zadeh AB. Improvements in comminution efficiency through high velocity impact. (M.Sc. thesis). Vancouver: University of British Columbia; 2012.
[78] Tasdemir A. Fractal evaluation of particle size distributions of chromites in different comminution environments. Miner Eng 2009;22:156–67.
[79] Svedensten P, Hulthén E. Fragmenteringsförsök för LKAB: Formbetingad krossning i inter particle breakage och single particle breakage försök. (MinBas Report). Gothenburg, Sweden: Chalmers University; 2005 (in Swedish).
[80] Metso Minerals Industries. Review of feed size distribution and mill operating parameters on the performance of the KA2 comminution circuit. Report to LKAB, Project no. LK01M. Metso Minerals Optimization Services; 2007.
[81] Tavares LM, das Neves PB. Microstructure of quarry rocks and relationships to particle breakage and crushing. Int J Miner Proc 2008;87:28–41.
[82] Okubo S, Chen WL, Fukui K. A consideration on particle size distribution of fragments and energy required in uniaxial compression tests. Shigen-to-sozai 2002;118–212:729–36.
[83] Kim DS. The effect of shock-induced damage on comminution of rock materials. (Ph.D. thesis). Salt Lake City: University of Utah; 1993.
[84] McCarter MK, Kim DS. Influence of shock damage on subsequent comminution of rock. In: Rossmanith HP, editor. Proceedings of the 4th international symposium on Rock Fragmentation by Blasting (FRAGBLAST 4), Vienna, 5–8 July 1993. p. 63–70.
[85] Lee E. Bergmaterialkarakterisering, interparticle breakage. Report Tillämpad mekanik. Göteborg, Sweden: Chalmers Tekniska Högskola; 2008 (in Swedish).
[86] Svedensten P, Lee E. Bergmaterialkarakterisering, interparticle breakage. Report Tillämpad mekanik. Göteborg, Sweden: Chalmers Tekniska Högskola; 2008 (in Swedish).
[87] Rager AH. The Interaction of rock and water during shock decompression: a hybrid model for fluidized ejecta formation. Paper 667. (Ph.D. thesis). Las Vegas: University of Nevada; 2010.
[88] Steiner HJ. The significance of the Rittinger equation in present-day comminution technology. In: Proceedings of the XVII international minerals processing congress, Dresden, Germany, 23–28 September 1991, vol. I; 1991. p. 177–88.
[89] Ouchterlony F. Fragmentation characterization; the Swebrec function and its use in blast engineering. In: Sanchidrián JA, editor. Proceedings of the 9th international symposium on Rock Fragmentation by Blasting (FRAGBLAST 9), Granada, Spain, 13–17 September 2009. Leiden: CRC Press/Balkema; 2011. p. 3–22.
[90] Matlab 7.13. Natick, MA: The MathWorks Inc; 2011.
[91] Coleman TF, Li Y. On the convergence of reflective Newton methods for large-scale nonlinear minimization subject to bounds. Math Program 1994;67(2): 189–224.
[92] Coleman TF, Li Y. An interior, trust region approach for nonlinear minimization subject to bounds. SIAM J Optim 1996;6(2):418–45.
[93] Lagarias JC, Reeds JA, Wright MH, Wright PE. Convergence properties of the Nelder–Mead Simplex method in low dimensions. SIAM J Optim 1998;9(1): 112–47.